Electronic Structures of Metal Hexacarbonyls

Nancy A. Beach and Harry B. Gray[1]

Contribution from the Department of Chemistry, Columbia University, New York, New York, and Contribution No. 3617 from the Gates and Crellin Laboratories of Chemistry, California Institute of Technology, Pasadena, California 91109. *Received January 31, 1968*

Abstract: Electronic spectra of neutral and ionic metal hexacarbonyls are reported. The spectra of $Cr(CO)_6$, $Mo(CO)_6$, and $W(CO)_6$ were measured in the vapor and solution states, the latter at both 300 and 77°K. The spectra of $V(CO)_6^-$, $Mn(CO)_6^+$, and $Re(CO)_6^+$ in solution at 300°K are reported with additional spectral measurements for $V(CO)_6^-$ at 77°K. The transition assignments and discussion of electronic structures are based on calculated molecular orbital energy levels for the various hexacarbonyls.

Bonding in transition metal carbonyls is of considerable theoretical interest to chemists because of the tendency of carbon monoxide to form complexes with metals in very low formal oxidation states. The availability of empty π-antibonding (π^*) orbitals apparently allows a strong metal–CO bond in the presence of low formal metal charge. This is possible because delocalization of electron density from the filled metal $d\pi$ orbitals into the CO π^* orbitals increases the attractive potential of the metal, giving rise to stronger d-orbital σ bonding than would be otherwise anticipated. The increased participation of the CO σ orbitals in turn produces an expansion of the metal orbitals, especially the d orbitals, and thus enhances overlap with both the π^b and the π^* CO orbitals. In this model, then, it is evident that the CO π^* orbitals play an important role in the stability of transition metal carbonyls.

Semiquantitative estimates of the degree of π bonding in metal carbonyls have been made from derived force constants of CO stretching modes.[2] Although these estimates serve as a very useful index, an independent basis for estimation of $M\rightarrow\pi^*CO$ bonding is highly desirable. A possible basis which has not been extensively explored is in molecular orbital calculations which have been correlated with ionization potential and electronic spectral data. Although electronic spectral data are scarce, the few results available indicate an important role for $M\rightarrow\pi^*CO$ bonding, because d–d bands in octahedral metal carbonyls occur at very high energies.[3] The very large values for the separation between $t_{2g}(\pi^*)$ and $e_g(\sigma^*)$ indicate either unusual stability for the t_{2g} orbitals or unusual instability for the e_g orbitals, or, more probably, some degree of both effects.

In a previous paper we presented vapor-phase and solution spectra measured for the chromium family hexacarbonyls at room temperature.[3] Because of the need for higher resolution electronic spectral data in furthering electronic structural studies of the metal carbonyls, we have undertaken low-temperature measurements of several important octahedral metal carbonyls. The results of solution and vapor-phase measurements at 300°K, and frozen-solution data at 77°K, are reported in this paper for $Cr(CO)_6$, $Mo(CO)_6$, and $W(CO)_6$; solution data only are presented for $V(CO)_6^-$, $Mn(CO)_6^+$, and $Re(CO)_6^+$. These spectra and the electronic structures of the hexacarbonyls are discussed in terms of their calculated molecular orbital energy levels.

Experimental Procedures

Preparation of Compounds. $Cr(CO)_6$, $Mo(CO)_6$, and $W(CO)_6$. Samples of these complexes were obtained from the Ethyl Corp. and the Climax Molybdenum Co. and purified by sublimation.

$[n\text{-}Bu_4N][V(CO)_6]$. An aqueous solution of $[n\text{-}Bu_4N]Br$ was deaerated with nitrogen. Alpha grade $[Na(diglyme)_2][V(CO)_6]$ was added to deaerated water and the resulting solution was filtered. Addition of the clear yellow filtrate to the $[n\text{-}Bu_4N]Br$ solution produced immediate precipitation of the yellow powder, $[n\text{-}Bu_4N][V(CO)_6]$, which was washed with N_2-saturated 95% ethanol and anhydrous ether. All operations were executed in a drybox. Solutions and solids containing $V(CO)_6^-$ are light and oxygen sensitive, decomposing to a yellow-green material (possibly containing the blue vanadyl ion). The decomposition of the solutions occurs within 0.5 hr if exposed to light. The infrared spectrum of the compound exhibits a single CO stretching band at 1864 cm^{-1} in acetonitrile solution.

$[Mn(CO)_6][BF_4]$. The sodium salt of manganese pentacarbonyl anion, $Na[Mn(CO)_5]$, was obtained by modification of the standard literature method.[4] The sodium amalgam was prepared in a 200-ml, three-necked flask fitted with a stirrer and a nitrogen gas outlet and attached to a nitrogen gas inlet and an oil pump through a nitrogen bubbler. The flask was also equipped with a large bore stopcock on the bottom for removal of the excess amalgam after completion of the reaction. Metallic sodium was freshly cut, weighed in paraffin oil, rinsed with pentane, dried, and slowly added to the triply distilled mercury, which was constantly stirred and flushed with nitrogen. When the amalgam cooled to room temperature, a 100-ml dropping funnel equipped with a pressure-equalizing arm and containing a solution of freshly sublimed dimanganese decacarbonyl, $Mn_2(CO)_{10}$, in tetrahydrofuran (THF), freshly distilled over lithium aluminum hydride, was added. Before dropwise addition of this solution to the amalgam, the entire system was thrice evacuated and filled with nitrogen. The amalgam was stirred constantly throughout the addition of the $Mn_2(CO)_{10}$ solution, and the entire mixture was stirred for about 45 min. Excess amalgam was removed from the solution, which was then washed with 2 ml of fresh mercury to remove any unreacted sodium. The stirrer was replaced by a stopper and the THF was removed by the oil pump, leaving the pale gray-green $Na[Mn(CO)_5]$ salt, subsequently used to prepare the ethyl manganese pentacarbonyl ester, $Mn(CO)_5CO_2C_2H_5$, in the following modification of the procedure of Kruck and Noack.[5] Great care must be taken to exclude air from contact with the $Na[Mn(CO)_5]$ as the slightest trace produces a reddish brown discoloration of the salt.

To the dry, solid $Na[Mn(CO)_5]$, about 15 ml of freshly distilled ethyl chloroformate and 30 ml of anhydrous ether were added drop-

(1) Author to whom correspondence should be addressed.
(2) (a) F. A. Cotton, *Inorg. Chem.*, **3**, 702 (1964); (b) F. A. Cotton and R. M. Wing, *ibid.*, **4**, 314 (1965).
(3) H. B. Gray and N. A. Beach, *J. Am. Chem. Soc.*, **85**, 2922 (1963).
(4) J. Kleinberg, Ed., "Inorganic Syntheses," Vol. VII, McGraw-Hill Book Co., Inc., New York, N. Y., 1963, p 198.
(5) T. Kruck and M. Noack, *Chem. Ber.*, **97**, 1693 (1964).

wise, and the resulting deep orange solution was stirred several hours. Attempts to remove the colorless $Mn(CO)_5CO_2C_2H_5$ by sublimation of the residual solution were unsuccessful, so the solution was filtered and methylene chloride was added to the resulting clear orange filtrate. Addition of gaseous BF_3 to this solution resulted in the immediate precipitation of the white fluoroborate salt of manganese hexacarbonyl cation, $[Mn(CO)_6][BF_4]$. The precipitate was washed thoroughly with freshly distilled THF and anhydrous ether. The infrared spectrum of the sample shows a single CO stretch at 2096 cm^{-1} in acetonitrile solution. Moisture must be excluded from contact with the cation, which forms $HMn(CO)_5$ immediately with H_2O.

Anal. Calcd for $[Mn(CO)_6][BF_4]$: C, 23.26; H, 0; F, 24.53. Found: C, 22.54; H, 0.08; F, 24.12.

$[Re(CO)_6][AlCl_4]$. $[Re(CO)_6][AlCl_6]$ was supplied by Dr. E. L. Muetterties, Central Research Department, Experimental Station, E. I. du Pont de Nemours and Co., Inc., Wilmington, Del. The compound is a white solid and is stable in the presence of H_2O and O_2, so no special care is required. A single CO stretching band was found at 2080 cm^{-1} in acetonitrile solution.

Physical Measurements. All visible and ultraviolet spectral data were obtained using a Cary Model 14 spectrophotometer; the cell compartment and associated equipment were flushed with nitrogen. Spectral grade solvents were used in all cases. For the vapor-phase measurements, a few small crystals of the freshly purified metal carbonyl were placed in a 10-cm quartz cell which was then stoppered. Acetonitrile solution spectra were measured with 1-cm quartz cells. Low-temperature spectral measurements were made on glasses formed by solution of the carbonyl in EPA, a commercial solvent mixture of ethanol, isopentane, and ethyl ether in the ratio 2:5:5 by volume, purchased from the Olin-Mathieson Co. or the Hartman-Leddon Co. The apparatus used for these measurements consisted of a Teflon-sleeved cell with quartz windows inserted into a metal cell holder fused to a dewar. The cell holder was then fitted into a quartz dewar equipped with optical windows. The spectrum was first measured on the metal carbonyl–EPA sample at room temperature, and then the sample was frozen carefully to a transparent glass over a period of 40 min using liquid nitrogen as the coolant. Immediately following these measurements on the carbonyl sample, the procedure was repeated for pure EPA, resulting in base-line curves at 300 and 77 °K which were subtracted from the first measurements on the carbonyl to correct for solvent absorption. The resulting low-temperature spectrum was then corrected for solvent contraction using the data of Passerani and Ross.[6] Gaussian analysis of the electronic spectra was performed as described elsewhere.[7]

Description of the Calculation

The octahedral geometry of $Cr(CO)_6$, $Mo(CO)_6$, and $W(CO)_6$ in both solid and vapor states has been confirmed by X-ray[8] and electron diffraction studies.[9] The linearity of the M–C–O sequence has also been established by these structural studies. Interatomic distances from electron diffraction studies on the vapors were used to calculate atomic overlaps. These distances are Cr–C = 1.92 ± 0.04 Å,[9] Mo–C = 2.06 ± 0.02 Å, and W–C = 2.07 ± 0.02 Å.[10] Bond-length data are not available for $Mn(CO)_6^+$, $V(CO)_6^-$, and $Re(CO)_6^+$. Thus we have estimated Mn–C and V–C to be 1.92 Å, and Re–C to be 2.07 Å. The metal basis set consists of the *n*d, (*n* + 1)s, and (*n* + 1)p orbitals. Richardson wave functions[11,12] for the neutral atom were used for the 3d, 4s, and 4p orbitals of V, Cr, and Mn; the p orbital functions were those for the $d^{n-1}p^1$ configuration. Analytical approximations[13] to the numerical Hartree–Fock–Slater wave functions for the metal of +1 charge were found to give more consistent results than those for the neutral atom in the case of Mo and W. For Re, the best results were obtained with the analytical approximations calculated by Dr. Harold Basch for the neutral Re of $d^5s^2p^0$ configuration.[14]

Wave functions for CO at the 1.16-Å internuclear distance observed in the complexes[9] were constructed by the SCCC method. Clementi double-ζ wave functions[15] were used for the atomic orbitals. From a basis set of 2s, 2pσ, and 2pπ orbitals for both carbon and oxygen, the 3σ, 4σ, 5σ, 6σ, 1π, and 2π MO's of CO were obtained. The 1σ and 2σ MO's were taken as the 1s orbitals of oxygen and carbon, respectively. The H_{ii}'s for both C and O were VOIP's evaluated as functions of charge and configuration.[16] Using the Mulliken population distribution[17] iteration to self-consistency gave $C^{+0.0625}\ 2s^{1.362}2p^{2.567}$, $O^{-0.0625}\ 2s^{1.629}2p^{4.433}$.[14]

The ground-state configuration of CO is $(1\sigma)^2(2\sigma)^2(3\sigma)^2(4\sigma)^2(1\pi)^4(5\sigma)^2$. For calculations on the metal complexes the 4σ, 5σ, 1π, and 2π MO's were taken as the ligand basis set. These MO's are designated σ_1, σ_2, π, and π^*, respectively, in the complexes.

Values of $-\epsilon$ for the σ_1, σ_2, and π MO's were equated with vertical ionization potentials derived from spectroscopic studies of CO.[18,19] Analysis of vibrational–rotational fine structure associated with observed band spectra for CO shows the 1π level to be more stable than the 5σ level. This assignment is further confirmed by photoelectron ionization studies[20] which distinguish electrons originating from nonbonding orbitals from those originating from bonding orbitals. In these studies the first ionization potential is found to be from a nonbonding orbital; consideration of the CO electronic structure shows the orbital must be of σ symmetry, because the π orbitals are either bonding or antibonding. The final $-\epsilon$ values taken for the occupied levels of CO are σ_2 = 113,000, π = 136,500, and σ_1 = 158,600 cm^{-1}.

Though vertical transition studies of CO indicate the π^* level is around $-48{,}000$ cm^{-1},[21] for the best correlation of calculated electronic structures with ionization potential and spectral data for the carbonyls π^* had to be treated as a parameter. For the group VIb hexacarbonyls the best value of $-\epsilon$ for π^* is $-33{,}000$ cm^{-1}. This result is entirely consistent with the expected destablization of the CO π^* level accompanying partial occupancy in the metal carbonyl.

(6) R. Passerani and I. G. Ross, *J. Sci. Instr.*, 30, 274 (1953).
(7) J. J. Alexander and H. B. Gray, *J. Am. Chem. Soc.*, 90, 4260 (1968).
(8) W. Rüdorff and U. Hofman, *Z. Physik. Chem.*, B28, 351 (1935).
(9) L. O. Brockway, R. V. G. Ewens, and M. W. Lister, *Trans. Faraday Soc.*, **34**, 1350 (1938).
(10) G. M. Nazarian, Ph.D. Thesis, California Institute of Technology, Pasadena, Calif., 1957, communicated by Dr. Richard E. Marsh.
(11) J. W. Richardson, W. C. Nieuwpoort, R. R. Powell, and W. F. Edgell, *J. Chem. Phys.*, **36**, 1057 (1962).
(12) J. W. Richardson, R. R. Powell, and W. C. Nieuwpoort, *ibid.*, **38**, 796 (1963).
(13) H. Basch and H. B. Gray, *Theoret. Chim. Acta*, 4, 367 (1966).
(14) Ligand wave functions, rhenium wave functions, metal–ligand group overlap expressions, eigenvectors, and eigenvalues have been deposited as Document No. 10041 with the American Documentation Institute, Auxiliary Publications Project, Photoduplication Service, Library of Congress, Washington 25, D. C. Copies may be secured by citing the document number and remitting in advance $2.50 for photoprints or $1.75 for 35-mm microfilm, payable to Chief, Photoduplication Service, Library of Congress.
(15) E. Clementi, "Tables of Atomic Functions," IBM, 1965.
(16) H. Basch, A. Viste, and H. B. Gray, *Theoret. Chim. Acta*, 3, 458 (1965).
(17) R. S. Mulliken, *J. Chem. Phys.*, **23**, 1833 (1955).
(18) F. H. Field and J. L. Franklin, "Electron Impact Phenomena and the Properties of Gaseous Ions," Academic Press Inc., New York, N. Y., 1957, p 110.
(19) B. Rosen, Ed., "Données Spectroscopiques Concernant les Molecules Diatomiques," Hermann and Cie, Paris, 1951, p 69.
(20) M. I. Al-Jobourg and D. W. Turner, *J. Chem. Soc.*, 4434 (1956).
(21) J. D. Simmons and S. G. Tilford, *J. Chem. Phys.*, **45**, 2965 (1966).

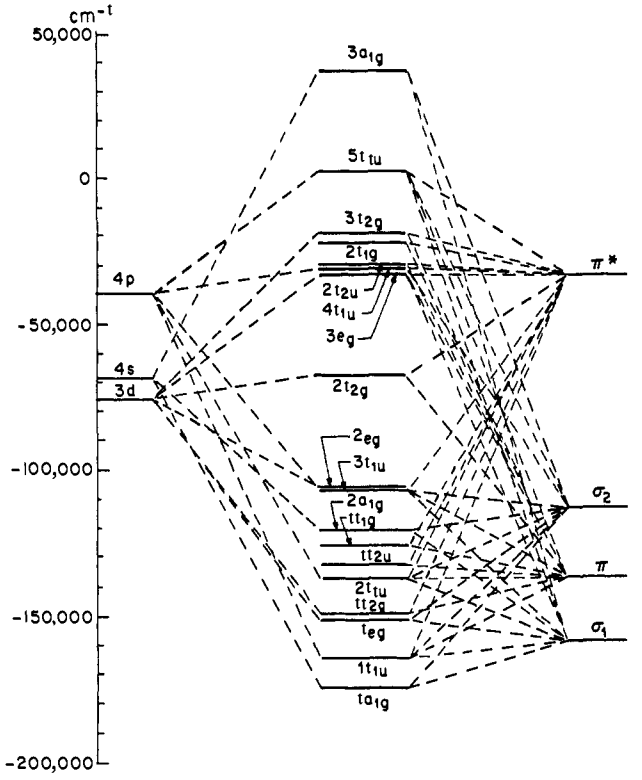

Figure 1. Molecular orbital energy level diagram for $Cr(CO)_6$.

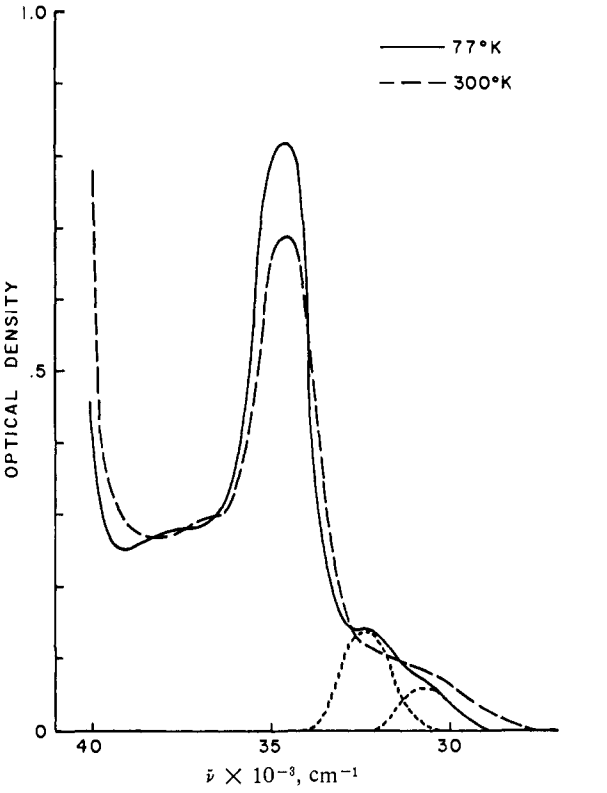

Figure 2. Electronic spectra of $Mo(CO)_6$ in EPA (0.55×10^{-4} M solution) at 300 and 77°K.

The metal H_{ii} were evaluated for specific fractional charges and configurations as outlined previously.[22] The H_{ij} were estimated as the arithmetic mean

$$H_{ij} = F_k G_{ij} \frac{(H_{ii} + H_{jj})}{2}$$

where the H_{ii}'s were uncorrected for ligand–ligand overlap and the F_k parameter was adjusted for the type of overlap involved. The group overlap integrals, G_{ij}, were calculated exactly from diatomic overlap integrals between SCF orbital functions expressed as linear combinations of Slater-type functions. The ligand H_{ii}'s were equated with the $-\epsilon$ values given for CO and corrected for ligand–ligand overlap. The F_k parameters were initially determined for the core group, the group VIb hexacarbonyls, by fitting closely the energy of the highest occupied MO with the first vertical ionization potential observed experimentally and approximating the separation of the $e_g(\sigma^*)$ and $t_{2g}(\pi)$ orbitals by the position of the lowest d–d band. The F_k factors calibrated on the neutral hexacarbonyls were then carried over for calculations of their respective isoelectronic neighbors.

The ligand combinations for O_h symmetry have been tabulated elsewhere.[3] The ligand H_{ii}'s were corrected for these overlaps by a factor appropriate for the arithmetic mean approximation used here.[23]

On the basis of the lanthanide contraction the same VOIP's were used for both second- and third-row transition elements. These VOIP's were estimated to be 10,000 cm^{-1} smaller than those for the analogous first-row element. For example, the A' and B' parameters for Cr were used for Mo and W whereas the C' parameters were reduced by a subtraction of 10,000 cm^{-1}. The same procedure was followed in the transition from Mn to Re.

The method of population analysis has been described previously.[7] An appropriate selection of results from the calculations is set out in Table I; all other input and output data are given elsewhere.[14] The energy level diagram for $Cr(CO)_6$ is representative of these calculations and is shown in Figure 1. A . . . $(2t_{2g})^6$ = $^1A_{1g}$ ground-state results in each case from filling in the 54 valence electrons, eight from each CO and six from the metal.

Electronic Spectra of $Cr(CO)_6$, $Mo(CO)_6$, $W(CO)_6$

The measured electronic spectra for $Cr(CO)_6$, $Mo(CO)_6$, and $W(CO)_6$ in vapor and solution media are reported and assigned in Table II. The most intense shoulder on the low-energy side of the first charge-transfer band in each case is assigned as the first spin-allowed d–d band, $^1A_{1g} \rightarrow {}^1T_{1g}$. The shoulder that appears between the two charge-transfer bands is not well resolved. It is attributed to the $^1A_{1g} \rightarrow {}^1T_{2g}$ transition, which should fall at approximately this position.

Support for the d–d assignments comes from spectral studies in EPA solutions and glasses at 300 and 77°K; the increased resolution at 77°K for $Mo(CO)_6$ and $W(CO)_6$ is shown in Figures 2 and 3, respectively. At low temperature, a decrease in the intensity of the broad shoulder on the low-energy side of the first charge transfer is observed, behavior characteristic of an orbitally forbidden transition. In addition to a decrease in intensity at 77°K, the shoulders in $Mo(CO)_6$ and $W(CO)_6$ are resolved into two and three components, respectively. The intensities of the two lower energy

(22) H. Basch, A. Viste, and H. B. Gray, *J. Chem. Phys.*, **44**, 10 (1966).
(23) The factor is $(1 + F_k Y_i)/(1 + Y_i)$, where $Y_i = \sum_{j \neq k} \sum c_{ij} c_{ik} G_{jk}$.

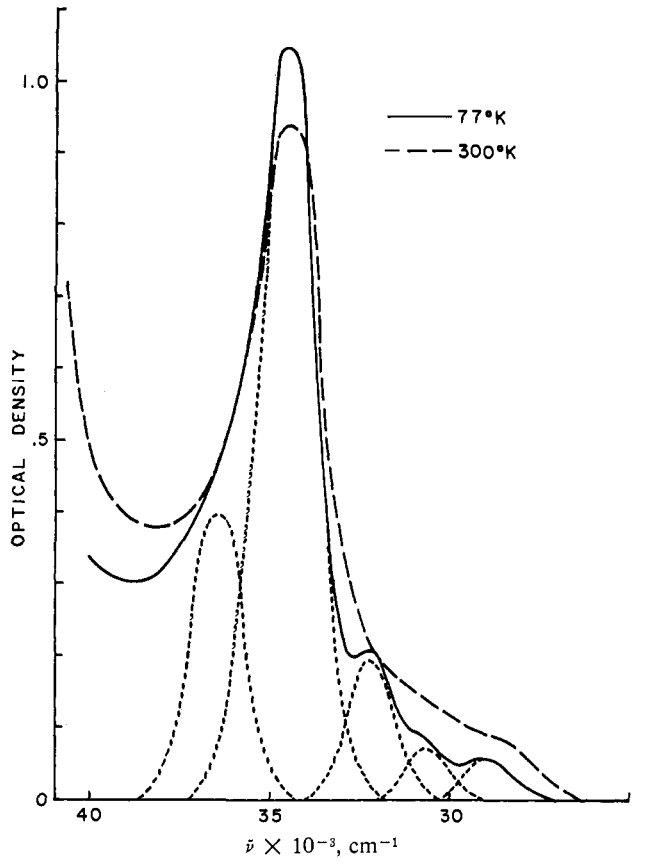

Figure 3. Electronic spectra of $W(CO)_6$ in EPA (0.80×10^{-4} *M* solution) at 300 and 77°K.

components are from one-half to one-third or less of those measured for the highest energy components. Gaussian analysis of room-temperature spectra of $Mo(CO)_6$ in the vapor and in acetonitrile and EPA solutions reveals a weak band at energies similar to those for the lowest energy band in $W(CO)_6$, thus supporting the similarity in electronic structure expected for both compounds.

The oscillator strengths measured for the two highest energy components are many times greater than those usually associated with spin-allowed, orbitally forbidden transitions; this may be understood in terms of their proximity to strongly allowed transitions. The separations of these two components in EPA at 77°K are 1650 and 1550 cm^{-1} for $Mo(CO)_6$ and $W(CO)_6$, respectively. These separations suggest that the bands should be assigned as vibrational structure arising from the t_{1u} CO stretching mode [the ground-state frequencies are 2000 cm^{-1} in $Cr(CO)_6$, 2004 cm^{-1} in $Mo(CO)_6$, and 1998 cm^{-1} in $W(CO)_6$, all in the vapor phase].[24] The vibrational splitting observed for the $^1T_{1g}$ excited state is smaller than the ~2000-cm^{-1} ground-state value, but the splitting cannot be obtained precisely. The values at room temperature in solution and vapor media are in the neighborhood of 1800 cm^{-1}.

Gaussian analysis of the $Cr(CO)_6$ spectrum at low temperature yields a weak band at 30,950 cm^{-1}; this band corresponds closely to the 30,700- and 30,600-cm^{-1} bands in $Mo(CO)_6$ and $W(CO)_6$, respectively, and is probably also part of the vibrational structure associated with the $^1A_{1g} \rightarrow {}^1T_{1g}$ transition.

(24) L. H. Jones, *Spectrochim. Acta*, **19**, 329 (1963).

The intensity of each of the lowest energy components in $Mo(CO)_6$ and $W(CO)_6$ relative to the other bands suggests assignment as a spin-forbidden d–d transition. A band of this type is not seen at all in $Cr(CO)_6$, and it is much weaker in $Mo(CO)_6$ than in $W(CO)_6$; this is just the behavior expected for a spin-forbidden d–d transition. Assignment of these lowest energy bands in $Mo(CO)_6$ and $W(CO)_6$ as the $^1A_{1g} \rightarrow {}^3T_{1g}$ transitions yields approximate *C* values of 1400 cm^{-1} for $Mo(CO)_6$ and 1300 cm^{-1} for $W(CO)_6$; these may be compared to the free atom values of 1794 cm^{-1} for Mo and 1887 cm^{-1} for W.[25] The observed reduction of *C* values is a very reasonable result in view of the degree of covalent bonding expected.

The two spin-allowed M→L charge-transfer bands are of extremely disparate intensity in each of the complexes investigated. The first bands have oscillator strengths of the magnitude (0.1) usually measured for transitions which are both spin and orbitally allowed, whereas the second bands have abnormally large (>1) oscillator strengths. Of the two antibonding MO's involved in these transitions, the $4t_{1u}$ level is stabilized through interaction with the metal p orbitals relative to the CO π^* level, whereas the pure ligand $2t_{2u}$ MO is destabilized relative to the CO π^* level by ligand–ligand interactions. The first charge transfer, $2t_{2g} \rightarrow 4t_{1u}$, is thus less of a "pure" M→L process than the second transition, the $2t_{2g} \rightarrow 2t_{2u}$, because of the admixture of metal character into the $4t_{1u}$ MO. According to this line of reasoning, a larger change in the electric dipole moment associated with each M–CO bond accompanies the $2t_{2g} \rightarrow 2t_{2u}$ transition.

It is interesting to examine the energy shifts in the charge-transfer bands on going from gas phase to solution. It is seen that, whereas the first charge-transfer band is relatively unperturbed by the solvent, the second band undergoes a red shift of the order of 1000 cm^{-1}. This behavior may be taken as evidence in favor of the assignments. An electron in the $2t_{2u}$ orbital is placed exclusively out on the CO's and should be more affected by solvent interactions than one in the "less exposed" $4t_{1u}$ level. We suggest that the $(2t_{2g})^5(2t_{2u})^1 = d^1T_{1u}$ state is particularly stabilized through favorable interaction with solvent dipoles; the result is lower energy in polar solvents for the second M→L transition.

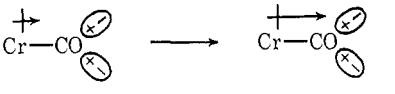

ground state excited state

Gaussian analysis of the acetonitrile and vapor-phase spectra yields a number of weaker bands on the high-energy side of the $^1A_{1g} \rightarrow d^1T_{1u}$ band. The presence of these weaker bands is indicated by the striking asymmetry of the high-energy half of the second charge-transfer band in $Mo(CO)_6$ and $W(CO)_6$; this is most marked in the latter case. In contrast to the heavier carbonyls, the second charge-transfer band in $Cr(CO)_6$ is more symmetric; only one rather weak band is resolved, at 50,900 cm^{-1}. The increasing asymmetry of the second charge-transfer band down the group VI hexacarbonyl family is most probably a reflection of the increasing importance of "spin-forbidden" bands. The

(25) J. S. Griffith, "The Theory of Transition-Metal Ions," Cambridge University Press, Cambridge, England, 1964, Appendix 6.

Table I. Selected Results of Molecular Orbital Calculations of Metal Hexacarbonyls (All Energies in 1000 cm^{-1})

	$Cr(CO)_6$	$Mo(CO)_6$	$W(CO)_6$	$V(CO)_6^-$	$Mn(CO)_6^+$	$Re(CO)_6^+$
			I. Metal H_{ii}			
d	−76.1	−74.1	−76.0	−69.2	−87.7	−81.7
s	−68.6	−64.0	−65.3	−65.4	−74.9	−67.9
p	−39.7	−35.4	−36.7	−38.5	−43.6	−37.1
			II. Ligand H_{ii} (corrected values in parentheses)			
$\sigma_1(a_{1g})$	158.6 (172.8)	158.6 (172.2)	158.6 (170.9)	158.6 (169.4)	158.6 (176.2)	158.6 (174.8)
σ_1 (e_g)	158.6 (150.2)	158.6 (151.0)	158.6 (151.7)	158.6 (152.2)	158.6 (148.2)	158.6 (149.5)
$\sigma_1(t_{1u})$	158.6 (157.6)	158.6 (157.8)	158.6 (157.9)	158.6 (157.8)	158.6 (157.3)	158.6 (157.7)
$\sigma_2(a_{1g})$	113.0 (126.6)	113.0 (126.6)	113.0 (125.4)	113.0 (123.4)	113.0 (129.8)	113.0 (129.4)
$\sigma_2(e_g)$	113.0 (104.4)	113.0 (104.8)	113.0 (105.6)	113.0 (106.4)	113.0 (102.3)	113.0 (103.3)
$\sigma_2(t_{1u})$	113.0 (111.5)	113.0 (111.8)	113.0 (111.9)	113.0 (111.8)	113.0 (111.1)	113.0 (111.6)
$\pi(t_{1g})$	136.5 (125.7)	136.5 (126.7)	136.5 (127.9)	136.5 (125.7)	136.5 (125.7)	136.5 (127.8)
$\pi(t_{1u})$	136.5 (140.7)	136.5 (140.1)	136.5 (139.6)	136.5 (140.7)	136.5 (140.7)	136.5 (139.6)
$\pi(t_{2g})$	136.5 (145.6)	136.5 (145.1)	136.5 (144.1)	136.5 (145.6)	136.5 (145.6)	136.5 (144.1)
$\pi(t_{2u})$	136.5 (132.6)	136.5 (133.2)	136.5 (133.6)	136.5 (132.6)	136.5 (132.6)	136.5 (133.6)
$\pi^*(t_{1g})$	33.0 (25.6)	33.0 (26.1)	33.0 (27.0)	33.0 (25.6)	33.0 (25.6)	33.0 (27.0)
$\pi^*(t_{1u})$	33.0 (36.0)	33.0 (35.6)	33.0 (35.3)	33.0 (36.0)	33.0 (36.0)	33.0 (35.3)
$\pi^*(t_{2g})$	33.0 (38.0)	33.0 (38.0)	33.0 (37.5)	33.0 (38.0)	33.0 (38.0)	33.0 (37.5)
$\pi^*(t_{2u})$	33.0 (30.1)	33.0 (30.4)	33.0 (30.8)	33.0 (30.1)	33.0 (30.1)	33.0 (30.8)
			III. Group Overlaps G_{ij}			
$G_{a_{1g}}(s,\sigma_1)$	−0.66917	−0.62996	−0.61723	−0.65091	−0.68304	−0.63864
$G_{a_{1g}}(s,\sigma_2)$	0.55721	0.61650	0.62460	0.52664	0.58458	0.62314
$G_{a_{1g}}(\sigma_1,\sigma_2)$	−0.24795	−0.20010	−0.19691	−0.24795	−0.24795	−0.19691
$G_{e_g}(d,\sigma_1)$	−0.34028	−0.30587	−0.32910	−0.37810	−0.30479	−0.26198
$G_{e_g}(d,\sigma_2)$	0.31114	0.30737	0.31816	0.32698	0.29275	0.30036
$G_{e_g}(\sigma_1,\sigma_2)$	0.15258	0.11616	0.11389	0.15258	0.15258	0.11389
$G_{t_{2g}}(d,\pi)$	0.19454	0.15545	0.17197	0.22777	0.16645	0.11659
$G_{t_{2g}}(d,\pi^*)$	0.31561	0.26310	0.28715	0.35940	0.27651	0.21068
$G_{t_{2g}}(\pi,\pi^*)$	0.08463	0.06856	0.06749	0.08463	0.08463	0.06749
$G_{t_{1u}}(p,\sigma_1)$	−0.23636	−0.52752	−0.51706	−0.22125	−0.25103	−0.55470
$G_{t_{1u}}(p,\sigma_2)$	0.15002	0.49175	0.50469	0.14150	0.15822	0.45294
$G_{t_{1u}}(p,\pi)$	0.31334	0.22295	0.20703	0.30849	0.31776	0.26086
$G_{t_{1u}}(p,\pi^*)$	0.33043	0.37564	0.35093	0.32082	0.33958	0.41513
$G_{t_{1u}}(\sigma_1,\sigma_2)$	0.02265	0.01461	0.01416	0.02265	0.02265	0.01416
$G_{t_{1u}}(\sigma_1,\pi)$	−0.09512	−0.07410	−0.07275	−0.09512	−0.09512	−0.07275
$G_{t_{1u}}(\sigma_1,\pi^*)$	−0.16510	−0.13073	−0.12849	−0.16510	−0.16510	−0.12849
$G_{t_{1u}}(\sigma_2,\pi)$	0.09088	0.07424	0.07312	0.09088	0.09088	0.07312
$G_{t_{1u}}(\sigma_2,\pi^*)$	0.15621	0.12960	0.12778	0.15621	0.15621	0.12778
$G_{t_{1u}}(\pi,\pi^*)$	0.04376	0.03172	0.03098	0.04376	0.04376	0.03098
$G_{t_{1g}}(\pi,\pi^*)$	−0.11163	−0.08530	−0.08365	−0.11163	−0.11163	−0.08365
$G_{t_{2u}}(\pi,\pi^*)$	−0.04181	−0.03020	−0.02950	−0.04181	−0.04181	−0.02950
			IV. F_k Parameters			
$F_{M\sigma}$	1.42	1.51	1.47	1.32	1.52	1.62
$F_{\sigma\sigma}$	1.42	1.51	1.47	1.32	1.52	1.62
$F_{M\pi}$	2.21	2.45	2.30	2.21	2.21	2.30
$F_{\pi\pi}$	2.21	2.45	2.30	2.21	2.21	2.30
$F_{\sigma\pi}$	2.00	2.00	2.00	2.00	2.00	2.00
			V. Metal Charge			
	+0.42	+0.56	+0.59	+0.39	+0.48	+0.58
			VI. Metal Population			
d	5.40	5.38	5.37	4.36	6.37	6.39
s	0.02	0.01	0.01	0.06	00.0	0.00
p	0.16	0.05	0.03	0.19	0.14	0.02
			VII. Ligand Population			
σ_1	2.06	2.05	2.05	2.07	2.04	2.04
σ_2	1.81	1.84	1.86	1.85	1.74	1.80
π	4.05	4.05	4.06	4.04	4.05	4.04
π^*	0.15	0.15	0.14	0.26	0.08	0.05
			VIII. Selected Eigenvalues			
$2t_{1u}$	−137.32	−137.47	−136.91	−137.43	−137.34	−137.01
$1t_{2u}$	−132.66	−133.21	−133.61	−132.66	−132.66	−133.61
$2a_{1g}$	−120.83	−121.19	−120.65	−119.67	−121.83	−122.33
$3t_{1u}$	−107.12	−108.18	−108.41	−107.88	−106.33	−107.77
$2t_{2g}$	−67.58	−68.14	−68.94	−60.51	−78.84	−77.52
$3e_g$	−33.16	−33.94	−34.31	−33.10	−35.46	−35.61
$4t_{1u}$	−31.06	−29.30	−29.09	−31.59	−31.32	−29.08
$2t_{2u}$	−29.66	−30.17	−30.54	−29.66	−29.66	−30.54

Table II. Electronic Spectra of $Cr(CO)_6$, $Mo(CO)_6$, and $W(CO)_6$ in Various Media[d]

Complex	Assignment	Vapor, 300°K[a]	EPA soln, 300°K[a]	EPA soln, 77°K[a]	Acetonitrile soln, 300°K[b]
$Cr(CO)_6$		50,900 (3.5)	*c*	*c*	>50,000
	$^1A_{1g} \rightarrow d^1T_{1u}$	44,200 (230)	*c*	*c*	43,600 (85,100; 227)
	$^1A_{1g} \rightarrow {}^1T_{2g}$	38,950 (3.7)	*c*	*c*	38,850 (3500; 4.0)
	$^1A_{1g} \rightarrow c^1T_{1u}$	35,800 (25)	35,800 (15)	35,950 (15)	35,700 (13,100; 24)
	$^1A_{1g} \rightarrow {}^1T_{1g}$	31,550 (3.7)	31,800 (1.8)	32,400 (1.6)	31,550 (2670; 3.3)
		29,000 (0.84)	30,000 (0.53)	30,900 (0.50)	29,500 (700; 0.61)
	$^1A_{1g} \rightarrow {}^3T_{1g}$	*c*	*c*	*c*	*c*
$Mo(CO)_6$		51,500 (28)	*c*	*c*	*c*
		47,500 (30)	*c*	*c*	46,500 (23,700; 37)
	$^1A_{1g} \rightarrow d^1T_{1u}$	43,950 (220)	*c*	*c*	42,800 (138,000; 230)
	$^1A_{1g} \rightarrow {}^1T_{2g}$	37,600 (10)	*c*	*c*	37,200 (7900; 8.4)
	$^1A_{1g} \rightarrow c^1T_{1u}$	34,900 (15)	34,550 (12)	34,700 (12)	34,600 (16,800; 17)
	$^1A_{1g} \rightarrow {}^1T_{1g}$	32,700 (2.2)	31,900 (1.9)	32,350 (1.8)	31,950 (2820; 2.7)
		30,950 (1.5)	30,000 (0.86)	30,700 (0.80)	30,150 (1690; 1.3)
	$^1A_{1g} \rightarrow {}^3T_{1g}$	29,350 (0.29)	28,100 (0.05)	*c*	28,850 (350; 0.21)
$W(CO)_6$		52,630 (7)	*c*	*c*	*c*
		50,350 (28)	*c*	*c*	49,000 (20,060; 25)
		47,350 (64)	*c*	*c*	46,350 (53,160; 67)
	$^1A_{1g} \rightarrow d^1T_{1u}$	44,600 (330)	*c*	*c*	43,750 (208,000; 300)
		39,000 (11)	*c*	*c*	39,550 (9600; 12)
	$^1A_{1g} \rightarrow {}^1T_{2g}$	36,650 (5.4)	*c*	*c*	37,100 (7400; 7.8)
	$^1A_{1g} \rightarrow c^1T_{1u}$	34,700 (18)	34,500 (11)	34,600 (12)	34,650 (17,600; 19)
	$^1A_{1g} \rightarrow {}^1T_{1g}$	31,950 (2.5)	31,850 (2.0)	32,150 (1.6)	31,850 (3250; 3.3)
		30,200 (1.3)	29,950 (0.91)	30,600 (0.57)	29,950 (1680; 1.3)
	$^1A_{1g} \rightarrow {}^3T_{1g}$	28,550 (0.78)	28,400 (0.57)	28,900 (0.50)	28,300 (1000; 0.83)

[a] In parentheses are $f \times 10^2$. [b] In parentheses are ϵ; $f \times 10^2$. [c] Not observed. [d] All energies in cm^{-1}.

Table III. Electronic Spectra of $V(CO)_6^-$, $Mn(CO)_6^+$, and $Re(CO)_6^+$ in Acetonitrile Solution

Complex	$\bar{\nu}$, cm^{-1}	ϵ	$f \times 10^2$	Assignment
$[n\text{-}Bu_4N][V(CO)_6]$	43,750	13,700	16	
	41,200	21,200	29	
	37,550	60,900	120	$^1A_{1g} \rightarrow d^1T_{1u}$
	~31,100	3,300	~3.2	$^1A_{1g} \rightarrow {}^1T_{2g}$
	28,400	6,240	8.0	$^1A_{1g} \rightarrow c^1T_{1u}$
	25,100	1,640	2.0	Vibrational components of
	23,200	300	0.28	$^1A_{1g} \rightarrow {}^1T_{1g}$
$[Mn(CO)_6][BF_4]$	49,900	27,000	61	$^1A_{1g} \rightarrow d^1T_{1u}$
	44,500	16,000	34	$^1A_{1g} \rightarrow c^1T_{1u}$
	~39,600	2,200	2	Vibrational components of
	~37,300	1,100	2	$^1A_{1g} \rightarrow {}^1T_{1g}$
	~33,250	600	1	$^1A_{1g} \rightarrow {}^3T_{1g}$
$[Re(CO)_6][AlCl_4]$[a]	51,200	77,900	158	$^1A_{1g} \rightarrow d^1T_{1u}$
	47,100	4,600	4	$^1A_{1g} \rightarrow {}^1T_{2g}$
	44,500	20,000	30	$^1A_{1g} \rightarrow c^1T_{1u}$
	40,700	2,900	2.9	Vibrational components of
	38,500	1,500	1.6	$^1A_{1g} \rightarrow {}^1T_{1g}$
	36,850	708	0.7	$^1A_{1g} \rightarrow {}^3T_{1g}$

[a] The absolute values of ϵ and f have large uncertainties due to the uncertainty in weighing the very small sample of pure material that was available. The relative values are quite accurate, however.

large intensities of these bands in $Mo(CO)_6$ and $W(CO)_6$ favor their assignment as spin-forbidden charge-transfer transitions. This assignment is not certain, however, because the calculations do show antibonding orbitals of even parity lying near the $2t_{2u}$ level; thus an alternative interpretation of these bands as orbitally forbidden charge-transfer transitions is also reasonable. The present experimental data do not allow final adjudication of this matter.

Electronic Spectra of Certain d^6 Ionic Hexacarbonyls: $V(CO)_6^-$, $Mn(CO)_6^+$, $Re(CO)_6^+$

Electronic spectral bands in acetonitrile solution and assignments for $[n\text{-}Bu_4N][V(CO)_6]$, $[Mn(CO)_6][BF_4]$, and $[Re(CO)_6][AlCl_4]$ are given in Table III. Figure 4 shows the EPA spectra at 300 and 77°K for $[n\text{-}Bu_4N][V(CO)_6]$; these band positions are set out in Table IV.

The electronic spectra of the ionic hexacarbonyls follow the general pattern of the neutral carbonyl

Table IV. Electronic Spectra of $[n\text{-Bu}_4N][V(CO)_6]$ in EPA Solution at 300 and 77°K

$\bar{\nu}$, cm^{-1} (300°K)	$\bar{\nu}$, cm^{-1} (77°K)	f(300° K)/ f(77°K)	Assignment
	31,150	*a*	$^1A_{1g} \rightarrow {}^1T_{2g}$
28,350	28,550	1.0	$^1A_{1g} \rightarrow c^1T_{1u}$
25,200	26,000	1.1	Vibrational components of
23,250	24,350	1.5	$^1A_{1g} \rightarrow {}^1T_{1g}$

[a] Band appears only in the 77°K spectrum.

spectra and analogous assignments have been made. The $^1A_{1g} \rightarrow c^1T_{1u}$ and $^1A_{1g} \rightarrow d^1T_{1u}$ transitions are noticeably affected by the differences in charge. These transitions occur at lowest energies in $V(CO)_6^-$ and move increasingly to higher energies as the charge on the central metal becomes more positive. This behavior is expected for M→L charge-transfer bands and may be taken as evidence of the correctness of the transition assignments.

Identification of the d–d bands has been done with the aid of a Gaussian analysis of the electronic spectral data. As in the case of the group VIb neutral hexacarbonyls, the spin-allowed bands appear only as broad shoulders, if they appear at all. Fortunately, the low-temperature spectrum of $V(CO)_6^-$ reveals a shoulder on the high-energy side of the $^1A_{1g} \rightarrow c^1T_{1u}$ transition, which in agreement with analogous spectral results for $Mo(CO)_6$ and $W(CO)_6$ is assigned as the $^1A_{1g} \rightarrow {}^1T_{2g}$ transition. Gaussian analysis of the shoulder on the low-energy side of this same charge-transfer transition resolves two bands separated by 1900 cm^{-1}. Since the CO stretching band in $V(CO)_6^-$ in acetonitrile occurs at 1864 cm^{-1}, these bands are assigned as vibrational components of the spin-allowed d–d transition, $^1A_{1g} \rightarrow {}^1T_{1g}$, in agreement again with similar structure observed for the neutral hexacarbonyls.

Ligand-field assignments for $Mn(CO)_6^+$ are obscured by the presence of only one weak shoulder at the low-energy end of a broad tail absorption from the two intense charge-transfer bands. A Gaussian analysis indicates that several bands make up the tail absorption; the high-energy bands in this system occur at 39,600 and 37,300 cm^{-1} and probably represent vibrational components of the $^1A_{1g} \rightarrow {}^1T_{1g}$ transition. Consistent with this interpretation is the fact that the CO stretching frequency in $Mn(CO)_6^+$ is found at 2096 cm^{-1} in acetonitrile solution. The second spin-allowed d–d band is expected to occur in the region between the two charge-transfer bands, but our Gaussian analysis failed to reveal it.

A Gaussian analysis of the $Re(CO)_6^+$ spectrum indicates the presence of the highest spin-allowed d–d band, $^1A_{1g} \rightarrow {}^1T_{2g}$, between the two charge-transfer bands in analogy with the neutral hexacarbonyls and $V(CO)_6^-$. The two highest energy bands of three resolved by analysis of the low-energy side of the first charge-transfer band are likely candidates for vibrational structure on the low-energy spin-allowed transition, $^1A_{1g} \rightarrow {}^1T_{1g}$, because their separation of 2200 cm^{-1} is close enough to the value of 2080 cm^{-1} measured for the CO stretching frequency in solution studies of $[Re(CO)_6][AlCl_4]$. These assignments for the spin-allowed d–d bands lead to a 16*B* separation of 7500 cm^{-1} which is larger than the 6200 cm^{-1} separation observed for

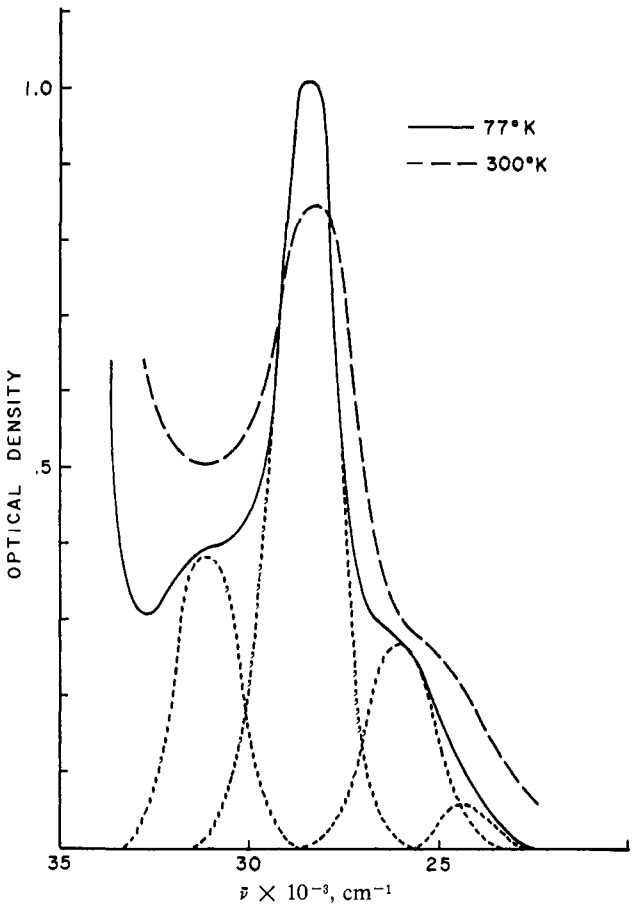

Figure 4. Electronic spectra of $[n\text{-Bu}_4N][V(CO)_6]$ in EPA at 300 and 77°K.

$W(CO)_6$. These values increase in the right direction since the free atom (ion) *B* value is larger for Re^+ than for W^0.[25] The considerable increase in energy of the d–d bands from $W(CO)_6$ to $Re(CO)_6^+$ is not unreasonable in view of the comparable shift in these bands from $Cr(CO)_6$ to $Mn(CO)_6^+$.

The lowest energy band in $Re(CO)_6^+$ may, like a similar one in $W(CO)_6$, be one of the spin-forbidden d–d transitions. In this case, the $^1A_{1g} \rightarrow {}^3T_{1g}$ transition would be the preferred assignment, giving a *C* value of 1375 cm^{-1}. The free-ion value of *C* for Re^+ is 1880 cm^{-1}.[26]

Discussion

Back-Donation in First-Row Complexes. It is clear from the large π^*CO populations in $2t_{2g}$ that back-donation plays a very significant role in the electronic structural description of all the metal hexacarbonyls. The situation is most pronounced for $V(CO)_6^-$; as illustrated in Table I, the calculations indicate that π back-donation accounts for the largest redistribution of electron density when this complex forms. That is, if the metal in its formal oxidation state is chosen as the reference point, there is *larger withdrawal* of negative charge from the metal through the π back-donation mechanism than the *total* of σ and π donation effects. As the positive charge on the central metal increases in an isoelectronic series, the degree of back-donation falls off sharply

(26) B. N. Figgis, "Introduction to Ligand Field Theory," Interscience Publishers, New York, N. Y., 1966, p 52.

and σ bonding assumes a larger role, as expected. Thus, the π*CO populations in $2t_{2g}$ are 0.24 in $V(CO)_6^-$, 0.13 in $Cr(CO)_6$, and 0.06 in $Mn(CO)_6^+$. This result is in agreement with the qualitative conclusion drawn from infrared data, because the $\nu_{t_{1u}}$(CO) values are 1864, 2000, and 2096 cm^{-1} for $V(CO)_6^-$, $Cr(CO)_6$, and $Mn(CO)_6^+$, respectively.

Table V. Extent of π Back-Bonding in Metal Carbonyl and Nitrosylcyanide Complexes

Complex	Molecular orbital	π* population	ν(A≡B), cm^{-1}
$V(CN)_5NO^{5-}$ [a]	6e	0.74 (π*NO)	1575
$V(CN)_5NO^{5-}$ [a]	$2b_2$	0.21 (π*CN)	2095
$V(CO)_6^-$	$2t_{2g}$	0.24 (π*CO)	1864
$Mn(CN)_5NO^{3-}$ [a]	6e	0.42 (π*NO)	1725
$Mn(CN)_5NO^{3-}$ [a]	$2b_2$	0.047 (π*CN)	2138
$Mn(CO)_6^+$	$2t_{2g}$	0.06 (π*CO)	2096

[a] P. T. Manoharan and H. B. Gray, *Inorg. Chem.*, **5**, 823 (1966).

It is of interest to compare the relative π-acceptor potential of NO^+, CN^-, and CO from the calculations available. Complexes in which fair comparison is possible include two isoelectronic pairs: $V(CN)_5NO^{5-}$, $V(CO)_6^-$; and $Mn(CN)_5NO^{3-}$, $Mn(CO)_6^+$. The calculated π* populations for CN^-, NO^+, and CO in these complexes are given in Table V. The data suggest that of the three NO^+ is by far the most effective π acceptor, the over-all order of π-acceptor ability being $NO^+ \gg CO > CN^-$.

Ionization Potentials and Charge-Transfer Energies. The metal hexacarbonyls are particularly well suited for electronic structural studies, because of the availability of extensive ionization potential data.[27] Assignments of the observed vertical ionization potentials based on the calculated energy levels for $Cr(CO)_6$, $Mo(CO)_6$, and $W(CO)_6$ are given in Table VI. The calculated positions of filled levels in the metal hexacarbonyls correspond remarkably closely to the "positions" obtained from experimental data. It is extremely encouraging that molecular orbital calculations calibrated using the lowest electronic transition and the first IP give such good agreement with the many additional ionization potentials.

The lack of metal orbital influence and the $2t_{2g} \rightarrow 2t_{2u}$ assignment for the second M→L band are confirmed by comparing the band positions with the measured vertical ionization potentials for $Cr(CO)_6$, $Mo(CO)_6$, and $W(CO)_6$. Since the vertical IP's pinpoint the $2t_{2g}$ level, the relative positions of the "pure" ligand level $2t_{2u}$ can be estimated in the three cases from the energies of the $2t_{2g} \rightarrow 2t_{2u}$ transition. This analysis places $2t_{2u}$ at 23,400 ± 600 cm^{-1} in every case; thus, consistent with theory, we find that the position of $2t_{2u}$ is not significantly affected by the central metal in an analogous series of complexes. The $4t_{1u}$ level, on the other hand, is metal sensitive because of admixture of central atom p orbitals. We shall make use of this result shortly.

Both the IP data and charge-transfer spectra show essentially the same orbital electronegativity for the

(27) (a) D. R. Lloyd and E. W. Schlag, to be submitted for publication; (b) D. W. Turner, C. Baker, and W. C. Price, to be submitted for publication.

Table VI. Orbital Energies and Vertical Ionization Potentials for Metal Hexacarbonyls

Complex	Orbital energies, calcd (1000 cm^{-1})		IP_{vert}, exptl[a] (1000 cm^{-1})
$Cr(CO)_6$	$2t_{2g}$	−67.6	67.8
	$2e_g$	−106.0	107.4
	$3t_{1u}$	−107.1	113.9
	$2a_{1g}$	−120.8	116.9
	$1t_{1g}$	−126.1	...
	$1t_{2u}$	−132.7	...
	$2t_{1u}$	−137.3	141.0
	$1t_{2g}$	−149.4	~149.2
$Mo(CO)_6$	$2t_{2g}$	−68.1	67.8
	$2e_g$	−107.6	105.7
	$3t_{1u}$	−108.2	113.3
	$2a_{1g}$	−121.2	117.8
	$1t_{1g}$	−127.1	122.0
	$1t_{2u}$	−133.2	...
	$2t_{1u}$	−137.5	142.2
	$1t_{2g}$	−149.0	...
			~157.3
$W(CO)_6$	$2t_{2g}$	−68.9	67.4
	$2e_g$	−108.2	106.7
	$3t_{1u}$	−108.4	113.9
	$2a_{1g}$	−120.6	117.3
	$1t_{1g}$	−128.1	121.9
	$1t_{1u}$	−133.6	...
	$2t_{1u}$	−136.9	142.0
	$1t_{2g}$	−147.9	...
			~157.3

[a] From ref 27b.

$2t_{2g}$ levels in $Cr(CO)_6$, $Mo(CO)_6$, and $W(CO)_6$. This behavior parallels that of $M(CN)_6^{3-}$ complexes, being in sharp contrast to the situation in MCl_6^{n-} complexes which show decreasing stability of t_{2g} in going from 3d to 5d central metal ions.[7] Since we expect some decrease in metal 4d and 5d orbital stability as compared with 3d, the constant orbital electronegativity of t_{2g} in the hexacarbonyls supports the idea of increasing M→π*CO bonding down the series. On the other hand, the calculations give very little difference in the population of π*CO for the three complexes in question.

Another factor of considerable interest is the extent to which the valence p orbitals are involved in π bonding in the three rows of transition metals. In the metal hexacarbonyls, our model suggests that the stability of the $4t_{1u}$ level relative to the reference point $2t_{2u}$ is proportional to the interaction of metal p orbitals (t_{1u}) with the $t_{1u}\pi$* ligand orbitals. Thus the $2t_{2u}$–$4t_{1u}$ separations give one measure of the relative participation of *n*p orbitals. From the vapor spectra, the $2t_{2u}$–$4t_{1u}$ separations are 8400 cm^{-1} in $Cr(CO)_6$, 9050 cm^{-1} in $Mo(CO)_6$, and 9900 cm^{-1} in $W(CO)_6$; this suggests that *n*p bonding increases in the order 4p < 5p < 6p. A similar conclusion may be extracted from the 5400 and 6700 cm^{-1} separations in $Mn(CO)_6^+$ and $Re(CO)_6^+$, respectively.

Ligand-Field Parameters. Table VII summarizes the values of Δ, *B*, and *C* derived from the electronic spectra of the hexacarbonyl complexes. It is interesting to note the large increase in Δ values with metal atomic numbers in an isoelectronic 3d or 5d series, that is $\Delta[Mn(CO)_6^+] > \Delta[Cr(CO)_6] > \Delta[V(CO)_6^-]$ and $\Delta[Re(CO)_6^+] > \Delta[W(CO)_6]$. This trend is in sharp contrast to the constancy of Δ in $Fe(CN)_6^{4-}$ and $Co(CN)_6^{3-}$. To explain the latter observation, we have argued[28] that

(28) J. J. Alexander and H. B. Gray, *Coordination Chem. Rev.*, **2**, 29 (1967).

Table VII. Ligand-Field Parameters (cm^{-1}) for the Metal Hexacarbonyls

Complex	Δ	B_{cpx}	$B_{free\ ion}$[a]	C	$\beta = B_{cpx}/B_{free\ ion}$
$V(CO)_6^-$	25,500	430	...	1300[b]	...
$Cr(CO)_6$	32,200	520	790	1700[b]	0.66
$Mn(CO)_6^+$	41,050	...	870	2600	...
$Mo(CO)_6$	32,150	380	460	1100	0.83
$W(CO)_6$	32,200	390	370	1300	1.1
$Re(CO)_6^+$	41,000	470	470[c]	1375	1.0

[a] From ref 25. [b] Estimated value. [c] From ref 26.

in the transition from Fe(II) to Co(III) the increased σ bonding destabilizes $3e_g\sigma^*$ to the same extent that $2t_{2g}$ is destabilized by the decreased $M\rightarrow\pi^*CN$ bonding; the result is a constant Δ. In the hexacarbonyls, as in $Os(CN)_6^{4-}$ and $Ir(CN)_6^{3-}$,[7] the evidence of increasing Δ values indicates that along an isoelectronic series as above, the σ bonding energetics are affected to a considerably greater extent than the analogous π bonding quantities.

Another effect of interest is the variation of Δ with ligand in an nd^5 or nd^6 series (n = 3–5). Several comparisons are shown in Figure 5. The percentage increase in Δ in going from 3d to 5d valence orbitals again depends on the type of ligand involved. For Cl^-, a very large fractional increase in Δ is observed; a substantial percentage increase in Δ is observed for NH_3, but Δ(CO) in one series actually shows a slight decrease. These observations are consistent with the above analysis, because interelectronic-repulsion effects should decrease in the order 3d > 4d > 5d. Thus, the π-donor ligand is able to move into a better d_σ overlap position as n increases with a resulting destabilization of the $3e_g\sigma^*$ level. The CO ligands, presumably, have already fully exploited the d_σ bonding for the lowest n value and have less to gain in the 4d and 5d series. Indeed, evidence from IP and charge-transfer spectral data (*vide supra*) indicates the $2t_{2g}$ level remains stationary down a series such as $M(CO)_6$ M = Cr, Mo, W). We infer from these data that the d_σ bonding actually decreases, and it is the increased π bonding in carbonyl complexes that holds Δ(4d) and Δ(5d) at values comparable to the Δ(3d) values.

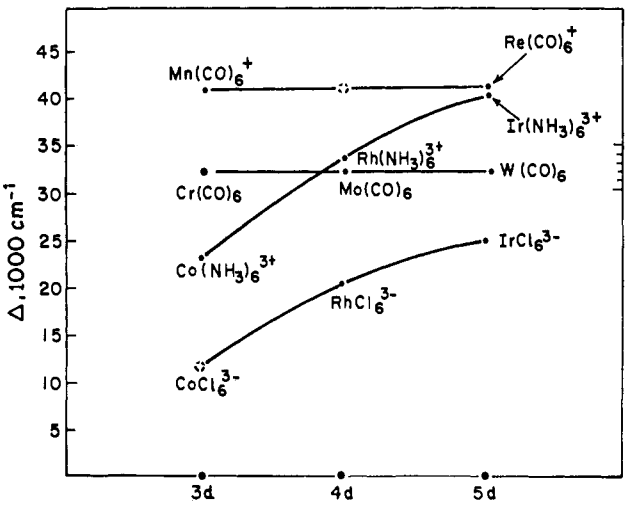

Figure 5. Dependence of Δ on the n quantum number of the d valence orbitals for octahedral complexes.

Acknowledgments. We thank the National Science Foundation for support of this research. Dr. Richard Marsh kindly communicated to us certain pertinent results from the Ph.D. thesis of G. M. Nazarian. We are grateful to Professor D. W. Turner and Dr. D. R. Lloyd for allowing us prepublication access to vertical ionization potential data for the metal hexacarbonyls. We thank Dr. E. Billig for help with the synthesis of $[Mn(CO)_6][BF_4]$ and for several useful discussions.

Electronic Structures of Square-Planar Complexes

W. Roy Mason, III, and Harry B. Gray[1]

Contribution No. 3664 from the Gates and Crellin Laboratories of Chemistry, California Institute of Technology, Pasadena, California 91109.
Received April 19, 1968

Abstract: Electronic spectra of several square-planar complexes of the type $[MX_4]^z$ (M = Pd(II), Pt(II), Au(III); X = Cl^-, Br^-, CN^-, NH_3) are reported in nonaqueous media at room and liquid nitrogen temperatures. In most cases the spectral resolution is considerably enhanced in the rigid, low-temperature glasses. Detailed assignments of spectra measured under carefully controlled conditions allow a comparison of electronic structures and energy levels in the various square-planar systems. The halide complexes show strong ligand→metal charge-transfer absorptions, the cyanides show metal→ligand bands, whereas the ammine complexes exhibit allowed d → p transitions. Trends in d–d and charge-transfer energies are discussed.

Recent investigations of the electronic structures of square-planar complexes indicate that the electronic energy levels vary according to the nature of the ligand.[2-4] The nature of the variation, however, is not presently clear. In view of the several theoretical

(1) Author to whom correspondence should be addressed.

(2) H. B. Gray and C. J. Ballhausen, *J. Am. Chem. Soc.*, **85**, 260 (1963).

(3) C. J. Ballhausen, N. Bjerrum, R. Dingle, K. Eriks, and C. R. Hare, *Inorg. Chem.*, **4**, 514 (1965).

(4) H. Basch and H. B. Gray, *ibid.*, **6**, 365 (1967).